Microbial Cell Factories

RESEARCH

Open Access

Genetic engineering of *E. coli* K-12 for heterologous carbohydrate antigen production

Caixia Li[1†], Hongxu Zha[1†], Ziyan Jiao[1†], Keyan Wei[1], Huaiyu Gao[1], Feiyi Lai[1], Zuoyong Zhou[1], Hongyan Luo[1*] and Pei Li[1*]

Abstract

Background Carbohydrate-based vaccines have made a remarkable impact on public health over the past three decades. Efficient production of carbohydrate antigens is a crucial prerequisite for the development of such vaccines. The enzymes involved in the synthesis of bacterial surface carbohydrate antigens are usually encoded by large, uninterrupted gene clusters. Non-pathogenic *E. coli* glycoengineering starts with the genetic manipulation of these clusters. Heterologous gene cluster recombination through an expression plasmid has several drawbacks, including continuous antibiotic selection pressure, genetic instability, and metabolic burdens. In contrast, chromosome-level gene cluster expression can minimize the metabolic effects on the host and reduce industrial costs.

Results In this study, we employed the suicide vector-mediated allelic exchange method to directly replace the native polysaccharide gene clusters in *E. coli* with heterologous ones. Unlike previously strategies, this method does not rely on I-SceI endonuclease or CRISPR/Cas system to release the linearized DNA insert and λ-red recombinase to promote its homologous recombination. Meanwhile, the vectors could be conveniently constructed by assembling multiple large DNA fragments in order in vitro. The scarless chromosomal insertions were confirmed by whole-genome sequencing and the polysaccharide phenotypes of all glycoengineered *E. coli* mutants were evaluated through growth curves, silver staining, western blot, and flow cytometry. The data indicated that there was no obvious metabolic burden associated with the insertion of large gene clusters into the *E. coli* W3110 O-antigen locus, and the glycoengineered *E. coli* can produce LPS with a recovery rate around 1% of the bacterial dry weight. Moreover, the immunogenicity of the heterologously expressed carbohydrate antigens was analyzed by mice immunization experiments. The ELISA data demonstrated the successful induction of anti-polysaccharide IgM or IgG antibodies.

Conclusions We have provided a convenient and reliable genomic glycoengineering method to produce efficacious, durable, and cost-effective carbohydrate antigens in non-pathogenic *E. coli*. Non-pathogenic *E. coli* glycoengineering has great potential for the highly efficient synthesis of heterologous polysaccharides and can serve as a versatile platform to produce next-generation biomedical agents, including glycoconjugate vaccines, glycoengineered minicells or outer membrane vesicles (OMVs), polysaccharide-based diagnostic reagents, and more.

Keywords Glycoengineering, DNA Long fragment editing, *E. coli* K-12, *S. enterica*, Polysaccharide biosynthesis

[†]Caixia Li, Hongxu Zha and Ziyan Jiao have contributed equally to this work.

*Correspondence:
Hongyan Luo
luohy511@swu.edu.cn

Pei Li
lipei98989@swu.edu.cn
[1] College of Veterinary Medicine, Southwest University, Chongqing 400715, China

Introduction

The outermost surface of bacteria is usually coated by a dense layer of carbohydrates [1, 2], which are millions of chain-length different polysaccharides forming a formidable barrier that prevents complement proteins or antibodies from accessing the innermost bacterial surface [3–5]. Not surprisingly, bacterial surface polysaccharides are attractive targets for subunit vaccine development [6]. For example, the application of commercial conjugate vaccines against the capsular polysaccharide of Haemophilus *influenzae* type b (Hib), pneumococcus, and serogroups C, A,W, and Y of meningococcus has dramatically decreased the disease rates over the last three decades [7, 8].

Before the development of any carbohydrate-based vaccines, the production of carbohydrate antigens is a prerequisite. Collectively, there are three strategies to produce these carbohydrate antigens: chemical synthesis [9], chemoenzymatic synthesis [10], and enzymatic biosynthesis [11–13]. At present, the biosynthesis method is much more cost-effective and scalable than the others. In terms of biosynthesis, polysaccharide antigens can be obtained from two distinct sources: natural sources [14] or engineered synthesis [15]. For instance, the polysaccharide antigens formulated in the commercial glycoconjugate vaccines mentioned above are mostly extracted from pathogenic bacteria [8]. However, large-scale bacterial fermentation of pathogenic bacteria is costly due to safety concerns and special cultural conditions. Meanwhile, reliance on natural sources of polysaccharide antigens would limit disease targets to those that are relatively easy to purify. Consequently, engineered approaches to carbohydrate production have become attractive alternatives [11, 16].

Bacterial surface polysaccharides are predominantly synthesized via the Wzx/Wzy-dependent pathway, which is conserved in both Gram-positive and Gram-negative bacteria [3]. For example, most polysaccharides are biosynthesized through the following basic steps: 1) generation of nucleotide sugar precursors; 2) sequential linkage of different sugars on undecaprenyl diphosphate (Und-PP) to form an Und-PP-linked repeating unit; 3) transportation of Und-PP-linked repeating unit from the cytoplasmic side to the periplasmic side by Wzx flippase; 4) polymerization of repeating units to a certain length by Wzy polymerase and Wzz chain-length regulator; 5) ligation of mature polysaccharide to a defined lipid donor by WaaL ligase [17, 18]. The major difference in bacterial polysaccharides lies in the structural variations within the repeat units, i.e., the nature, order, and linkage of the different sugar residues, which are also reflected by their genetic variations [17]. Fortunately, the genes involved in polysaccharide biosynthesis are typically clustered in a specific chromosomal locus [19, 20], which means transferring the gene cluster as a whole is typically enough to reinitiate the biosynthesis of these heterologous glycan structures. In summary, those fundamental findings have largely paved the way for bacterial glycoengineering, featuring in heterogeneous expression of polysaccharides in non-pathogenic *E. coli*.

An inevitable issue for the application of *E. coli* glycoengineering is the genetic manipulation of the polysaccharide gene cluster, either cloned into a recombinant plasmid [21] or inserted into the chromosome [13, 15]. The recombinant expression of large gene clusters via a plasmid has various limitations. For example, standard expression plasmids are often genetically unstable after the insertion of large DNA fragments. Although large DNA inserts could be accommodated in a limited number of cosmids or fosmids, which maintain the stability of large DNA fragments through various mechanisms, this approach often imposes a deleterious metabolic burden on a host, manifesting as a decrease in fitness [22]. Additionally, a significant disadvantage of using plasmids lies in the requirement of selection pressure to preserve the gene cluster within cells. This selection pressure necessitates the employment of antibiotics, which is undesirable for producing medicinal products as it poses a risk of allergic reactions to antibiotics and elevates manufacturing costs. Chromosomal insertion of large DNA fragments does not have these disadvantages. They are genetically stable, have no antibiotic selection markers, and maintain a minimum fitness cost [15]. The main obstacle to this strategy is the lack of methods for chromosomal insertion of such large DNA fragments.

Currently, few reports have successfully inserted DNA fragments larger than 10 kbp at desired loci on host cell genomes, but they all rely on the λ red recombinase of the λ phage [13, 15]. In this paper, we expand the toolkit of chromosomal insertion of large DNA fragments with another option. Using in vitro Gibson assembly methods [23], we were able to assembly the bacterial surface polysaccharide gene cluster into a suicide plasmid backbone. Following a conventional double cross-over homologous recombination [24], the non-essential glycan gene clusters in *E. coli* K-12 strains could be directly replaced by heterologous gene clusters. Moreover, this method could result in scarless insertion mutations. To facilitate the selection process and increase the positive mutants, a cassette of antibiotic resistance gene flanked by two FRT (FLP recognition target) sites could be fused after the heterologous gene clusters [25]. The antibiotic resistance gene would ultimately be deleted with the help of FLP

recombinase, leaving a single FRT scar right behind the inserted fragment [26].

Materials and methods

Bacteria, plasmids, and culture conditions

The bacteria and plasmids used in this study are listed in Table 1. *E. coli* and *S. enterica* strains were aerobically grown at 37 °C in Luria–Bertani (LB) broth or on LB agar. M9 minimal media with 0.4% (wt/vol) glucose was used to assess its potential for large-scale bacterial production at a relatively low cost [27]. All *E. coli* mutants were derived from the non-pathogenic *E. coli* K12 strain W3110. *sacB* gene-based counter selection in allelic exchange experiments was performed on LB agar containing 10% sucrose with no added sodium chloride and grown at 30 °C. Selection media were supplemented with 25 μg/mL chloramphenicol, 25 μg/mL kanamycin, or 50 μg/mL ampicillin. Diaminopimelic acid (DAP) (50 μg/mL) was added for the growth of the χ7213 strain [28, 29]. Electrocompetent *E. coli* or *S. enterica* cells were prepared as described previously [30]. In vitro growth rates of *E. coli* were determined by optical density measurements.

Bacterial growth assays were conducted using a Corning Costar 96-well flat-bottom EIA/RIA plate (REF 3590) in a SpectraMax iD3 plate reader (Molecular Devices). Overnight cultures were diluted at a ratio of 1:100 into 25 mL of LB broth or M9 minimal media, with or without

Table 1 Bacterial strains and plasmids used in this study

Strain or Plasmids	Description	Source
Strains		
S356	*S.* Paratyphi A	[32]
S100	*S.* Typhimurium	[32]
S246	*S.* Enteritidis	[32]
S229	*S.* Typhi	[31]
K028	*E. coli* W3110	Lab stock
K062	*E.coli* W3110 Δ*wecA*	Lab stock
χ7232	*E. coli endA1 hsdR17* (r_K-, m_K+) *glnV44 thi-1 recA1 gyrA relA1 Δ(lacZYA-argF)U169 λpir deoR* (φ*80dlac* Δ(*lacZ*)*M15*)	[32]
χ7213	*E. coli thi-1 thr-1 leuB6 glnV44 fhuA21 lacY1 recA1 RP4-2-Tc*::Mu λ*pir* Δ*asdA4* Δ*zhf-2*::Tn*10*	[32]
L0149	*E. coli* W3110 ΔOAg::*viaB*_locus	This study
L0137	*E. coli* W3110 Δ*wecA* ΔOAg::OAg^{SA}	This study
L0166	*E. coli* W3110 Δ*wecA* ΔOAg::OAg^{SA}, pET9a-wzy^{ST}	This study
L0169	*E. coli* W3110 Δ*wecA* ΔOAg:: OAg^{SA}, pET9a- (*wzy-wzzB*)ST	This study
L0136	*E. coli* W3110 Δ*wecA* ΔOAg::OAg^{ST}	This study
L0167	*E. coli* W3110 Δ*wecA* ΔOAg::OAg^{ST}, pET9a-wzy^{ST}	This study
L0170	*E. coli* W3110 Δ*wecA* ΔOAg::OAg^{ST}, pET9a- (*wzy-wzzB*)ST	This study
L0133	*E. coli* W3110 Δ*wecA* ΔOAg:: OAg^{SE}	This study
L0168	*E. coli* W3110 Δ*wecA* ΔOAg::OAg^{SE}, pET9a-wzy^{ST}	This study
L0171	*E. coli* W3110 Δ*wecA* ΔOAg::OAg^{SE}, pET9a- (*wzy-wzzB*)ST	This study
Plasmids		
pCP20	FLP^+, λ $cI857^+$, λ PR Rep^{ts}, Ap^R, Cm^R	[26]
pCP3	FRT-Cm-FRT cassette, Cm^R	[26]
pHY093	pRE112-Cm-GFP, *sacB*, mobRP4, R6K ori, Cm^R	Lab stock
pHY094	pRE112-Km-GFP, *sacB*, mobRP4, R6K ori, Km^R	Lab stock
pHY095	pRE112-Cm-ΔOAg	This study
pHY129	pRE112-Cm-ΔOAg::*viaB*_locus	This study
pHY099	pRE112-Km-ΔOAg::Cm_FRT2	This study
pHY100	pRE112-Km-ΔOAg::OAg^{ST}-Cm_FRT2	This study
pHY101	pRE112-Km-ΔOAg::OAg^{SE}-Cm_FRT2	This study
pHY102	pRE112-Km-ΔOAg::OAg^{SA}-Cm_FRT2	This study
pHY116	pET9a-wzy^{ST}	This study
pHY118	pET9a- (*wzy-wzzB*)ST	This study

the addition of antibiotics. The cultures were incubated at 37 °C with shaking at approximately 220 rpm, and the absorbance at 600 nm (A600) was recorded every 30 min for approximately 8 h. Each strain was cultured in triplicate to obtain an average A600 value at each time point.

Molecular and genetic manipulation

Bacterial mutagenesis was performed as previously described with few adaptations [31]. Suicide vectors and primers used in this study are listed in Table 1 and Supplemental Table S1, respectively. The gene cluster insertion mutations on the *E. coli* chromosome were constructed using the sucrose counter-selectable pRE112 (addgene, plasmid #43,828) suicide vectors [24]. Schematic maps of the relevant suicide plasmids and gene cluster insertion mutations in this study are illustrated in Figs. 1 and 2. A detailed description of the construction processes of these vectors can also be found in the Supplemental materials.

For scarless insertion mutation, two homologous arms (HA), the upstream (HA_UP) and downstream (HA_down) of the insertion locus, were amplified using

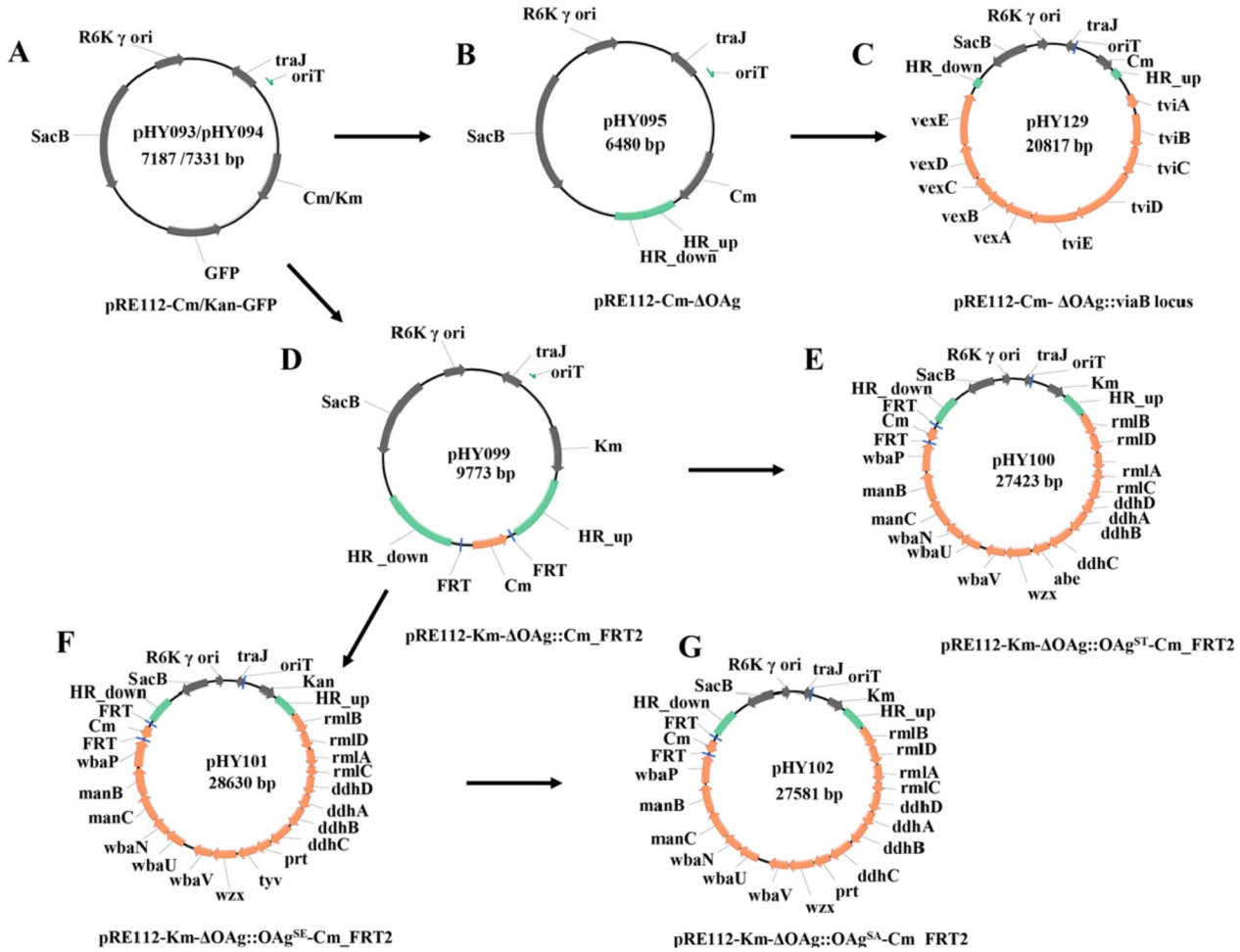

Fig. 1 Schematic map of suicide vectors. **A** All suicide vectors were derived from pHY093 (pRE112-Cm-GFP) or pHY094 (pRE112-Kan-GFP). **B** Two homologous arms, i.e., HA_up and HA_down were cloned from *E. coli* W3110 genome and fused together by fusion PCR. The fused homologous arms replaced the GFP cassette in pHY093 (pRE112-Cm-GFP), resulting in pHY095 (pRE112-Cm-ΔOAg). **C** the *viaB*_locus was cloned from *S.* Typhi genome. The linearized pHY095 (pRE112-Cm-ΔOAg) vector and *viaB*_locus were assembled in vitro, resulting in pHY129 (pRE112-Cm-ΔOAg::viaB locus). **D** A cassette of FRT-flanked chloramphenicol resistance gene was cloned from pCP3, and cloned into the middle of homologous arms, resulting in pHY099 (pRE112-Km-ΔOAg::Cm_FRT2). **E** The OAg^{ST} O-antigen gene cluster was cloned from *S.* Typhimurium genome via Long-range PCR. The linearized pHY099 (pRE112-Km-ΔOAg::Cm_FRT2) vector and OAg^{ST} were assembly in vitro, resulting in pHY100 (pRE112-Km-ΔOAg::OAg^{ST}-Cm_FRT2). **F** The OAg^{SE} O-antigen gene cluster was cloned from *S.* Enteritidis genome via Long-range PCR. The linearized pHY099 (pRE112-Km-ΔOAg::Cm_FRT2) vector and OAg^{SE} were assembly in vitro, resulting in pHY101 (pRE112-Km-ΔOAg::OAg^{SE}-Cm_FRT2). **G** pHY102 (pRE112-Km-ΔOAg::OAg^{SA}-Cm_FRT2) was derived from pHY101 by deliberately deleting the *tyv* gene

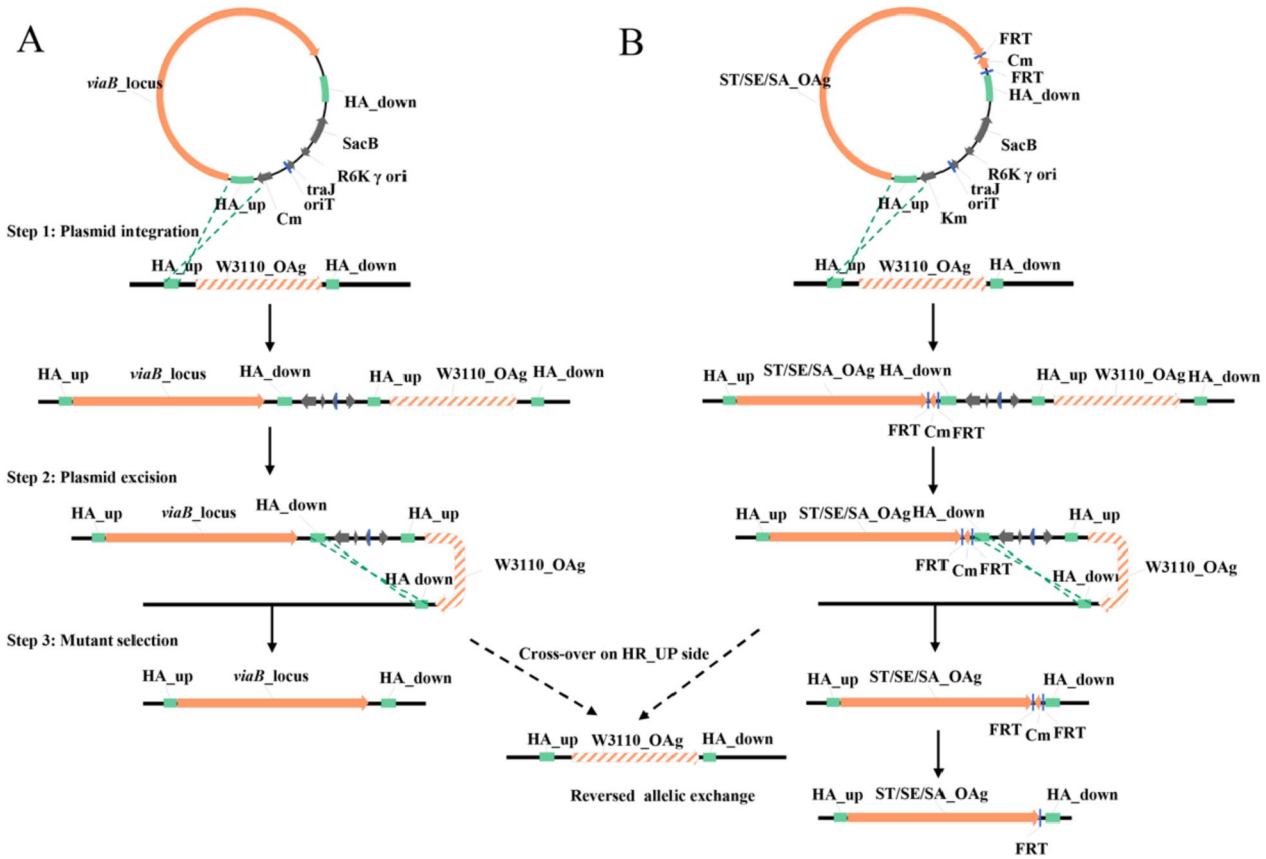

Fig. 2 General outline of the Chromosomal-level gene cluster insertion mutations. **A** Scarless insertion mutation. Successful mutations are achieved by consecutive single-crossovers. Step 1: The Suicide plasmid integrates into the chromosome of *E. coli* W3110 by a first cross-over recombination on either side of HA_up or HA_down. The schematic diagram only takes the cross-over on HA_up side as an example, while cross-over on HA_down side is similar. Plasmid integrated intermediate strains are selected on chromosomal plates. Step 2: The suicide plasmid is excised from the chromosome by a second cross-over recombination on HA_down side. Notably, cross-over recombination on HA_up side will lead to reversion allelic exchanges. All plasmid excised derivatives, i.e., either successful or reversed allelic exchange, are selected on sucrose plates. Positive mutants are screened by colony PCR and later sequenced by whole genome sequencing. **B** Insertion mutation with a single FRT scar. A cassette of FRT-flanked chloramphenicol resistance gene is fused immediately after the heterologous gene cluster to facilitate the selection process and increase the positive mutant rate. At step 1, plasmid integrated intermediate strains are selected on kanamycin plates. At step 3, plasmid excised derivatives are selected on sucrose plus chloramphenicol plates. The chloramphenicol will eliminate all reversion allelic exchange derivatives, and the chromosomal resistance gene could be later deleted by FLP recombinase, leaving a single FRT scar on the genome

PrimeSTAR Max DNA Polymerase (TaKaRa). After purification, these two fragments were fused by fusion PCR and cloned into the pHY093 (pRE112-Cm-GFP) or pHY094 (pRE112-Km-GFP), resulting in an intermediate vector. Polysaccharide gene clusters were amplified using PrimeSTAR GXL DNA Polymerase (TaKaRa) and assembled into the intermediate vector using Gibson Assembly Master Mix according to the manufacturer's instructions (New England BioLabs). The successful recombinant suicide vectors had the polysaccharide gene clusters flanked by the homologous arms. All assembly processes were screened in χ7232 host strain. The conjugational transfer of recombinant suicide vectors to *E. coli* W3110 was performed using the suicide vector donor strain χ7213. The first homologous recombination event (positive selection) was selected on chloramphenicol agar. The second homologous recombination event (negative selection), resulting in the excision of the suicide vector from the *E. coli* W3110 chromosome, was selected on 10% sucrose LB plates without sodium chloride and grown at 30 °C. Successful gene cluster insertion mutations were confirmed by PCR screening and whole genome DNA sequencing.

To increase the positive results after the second homologous recombination event, a minor improvement could be applied. A cassette of antibiotic resistance gene flanked by two FRT sites was fused immediately after the gene cluster on the suicide plasmid backbone. The other

procedures were identical to those previously described, with the exception that the second homologous recombination event was selected on LB plates containing 10% sucrose and the appropriate antibiotics, also without the inclusion of sodium chloride. After the PCR screening, a pCP20 plasmid was electroporated into the insertion mutants to excise the antibiotic resistance gene, leaving a single FRT scare right behind the inserted gene clusters. The pCP20 is easily curable when grown at 42 ℃.

In addition to the gene cluster insertion mutations, two plasmids were constructed for the proper polysaccharide synthesis and phenotype evaluation, namely pET9a-*wzy*ST and pET9a- (*wzy-wzzB*)ST. The DNA sequence of *wzy* and *wzzB* were from *S*. Typhimurium, and for clarity, (*wzy-wzzB*)ST means the *wzy* and *wzz* genes were fused in frame. It should be noted that the *wzy*ST or (*wzy-wzzB*)ST was flanked by approximately 200 bp upstream and downstream DNA sequences of *E. coli* W3110 *wzy* locus, and consequently, the expression of *wzy*ST or (*wzy-wzzB*)ST gene was not driven by the T7 promoter of the pET9a. The expression cassette of *wzy*ST and (*wzy-wzzB*)ST were directly synthesized and cloned into the commercialized pET9a vector by GenScript. The detailed DNA sequences of pET9a-*wzy*ST and pET9a- (*wzy-wzzB*)ST are revealed in Supplementary Table S2.

Polysaccharides silver staining and western blot

LPS silver staining was prepared, separated, and visualized using the method provided by Hitchcock and Brown [33]. For western blot, anti-O-antigen single-factor rabbit antisera (BD Biosciences) or anti-Vi polymer rabbit antisera (BD Biosciences) were used to probe the blots in PVDF membranes. The membranes were then incubated with anti-rabbit or anti-mouse horseradish peroxidase (HRP)-conjugated antibodies (Bioworld). Patterns were detected by the enhanced chemiluminescence (ECL) solution (Thermo Fisher Scientific).

LPS production

LPS isolation with high purity was achieved by the Proteinase K Digested, Phenol–Water Extraction method [34]. Briefly, lyophilized bacterial cells were resuspended in 15 mL of 10 mM Tris–Cl buffer (pH 8.0) containing 2% SDS, 4% 2-mercaptoethanol, and 2 mM $MgCl_2$. The suspension was vortexed and incubated at 65 °C until complete cell lysis. Proteinase K (1 mL of 100 μg/mL in solubilization solution) was added, followed by sequential incubations at 65 °C [1 h] and 37 °C (overnight). To precipitate LPS, 2 mL of 3 M sodium acetate and 40 mL of cold absolute ethanol were added to the digested suspension, followed by overnight incubation at −20 °C. After centrifugation (4,000 × g, 15 min), the pellet was washed twice by resuspension in 9 mL distilled water, reprecipitation with 1 mL 3 M sodium acetate and 20 mL ethanol, and incubation at −20 °C. The final pellet was dissolved in 9 mL of 10 mM Tris–Cl (pH 7.4) and treated with DNase I (0.5 mL, 100 μg/mL) and RNase (0.5 mL, 25 μg/mL) at 37 °C for 4 h. The mixture was heated to 65 °C for 30 min, mixed with an equal volume of preheated 90% phenol, and incubated at 65 °C (15 min). After cooling on ice, the aqueous layer was separated by centrifugation (6,000 × g, 15 min). The phenol phase was re-extracted with water, heated, and centrifuged again. Combined aqueous phases were dialyzed (3000 Dalton molecular weight cut off) against distilled water (48 h, multiple exchanges) and lyophilized for mass determination. LPS purity was analyzed by SDS-PAGE (Silver and Coomassie Staining) and spectrophotometry A260/A280 measurements.

Flow cytometric analysis

Flow cytometric analysis of glycoengineered *E. coli* was performed as described [35]. Briefly, overnight cultures of each strain were grown in LB broth with or without relevant antibiotics. The following day, the cultures were diluted 1:100 into 5 mL of LB broth and grown until the OD_{600} reached 0.6. Subsequently, 250 μL of the culture was centrifuged at 5000 rpm for 5 min, the supernatant was discarded, and the pellet was resuspended in 1 mL of PBS. This washing step was repeated twice. The bacterial outer membrane polysaccharide was detected using O-antigen signal-factor rabbit antiserum or Vi capsule rabbit antiserum (BD Biosciences), followed by a FITC-conjugated goat anti-rabbit secondary antibody (Abmart). The primary and secondary antibodies were diluted at 1:200 and 1:1000 in PBS, respectively. Then, 500 μL of the diluted antibodies was added to the sample, which was incubated at 37 °C for 30 min. After incubation, the cells were centrifuged again at 5000 rpm for 5 min, washed, and resuspended in 1 mL of PBS. The resuspended cells were analyzed using flow cytometry (FongCyte, Beijing Challen Biotechnology Co., Ltd) and FlowJo V10 software.

Whole-cell inactivated antigen preparation

0.5% (v/v) formalin was applied to prepare bacterial whole-cell inactivated antigens. Briefly, the bacteria were grown in LB broth at 37 °C with shaking until the OD_{600} value reached 0.9. The cultures were then harvested by centrifugation at 3000 × g for 10 min. PBS buffer was used to resuspend the bacterial pellet. A final concentration of 0.5% (v/v) formalin was added to the bacteria resuspension and mixed thoroughly overnight. A small aliquot of bacteria antigen was plated on LB agar and incubated overnight at 37 °C to verify the inactivation efficacies.

The inactivated bacterial cells were washed three times with sterile PBS to remove residual formalin and the final bacterial pellet was resuspended in PBS to 10^9 CFU/mL for immunization.

Mice immunization

Six-week-old female BALB/c mice were purchased from SJA Laboratory Animals Co., Ltd (Hunan, China). Two immunization schedules were conducted parallelly. The first one prepared the inactivated bacterial antigens with no adjuvants, while the second one prepared them with Complete Freund's Adjuvant (CFA) and Incomplete Freund's Adjuvant (IFA). For non-adjuvant preparation plan, six mice per group were subcutaneously injected at the tail base on day 0, and the injection volume per mouse was 100 µL in total containing approximately 10^8 inactivated bacterial cells. On days 14 and 28, the same booster dose was administered. For adjuvant preparation plan, all immunization processes were similar to the non-adjuvant one, except that the inactivated bacteria cells were mixed in advance with an equal volume of CFA in the primary immunization step and with an equal volume of IFA in the booster immunization steps. On day 35, blood samples were collected from the mice via the retro-orbital plexus, and the serum was collected after centrifugation at 2000 × g for 10 min at 4 °C. On day 42, mice were challenged orally with 5×10^7 CFU of *S.* Typhimurium and *S.* Enteritidis (~ 100 times LD_{50}), or intraperitoneally with 1×10^4 CFU of *S.* Typhi and *S.* Paratyphi A (~ 100 times LD_{50}). *S.* Typhimurium or *S.* Enteritidis was prepared by suspending the bacteria with sterile PBS, while *S.* Typhi and *S.* Paratyphi A were prepared by suspending the bacteria in 5 to 10% (wt/vol) hog gastric mucin [36].

Measurement of specific serum antibodies

S. Typhimurium and *S.* Enteritidis LPS were purchased from Sigma (St. Louis, MO, USA). *S.* Paratyphi A LPS was purified as described previously [34]. Microtiter plates were coated with *S. enterica* LPS or whole-cell inactivated *S.* Typhi. Serum IgM and IgG antibodies specific to *S. enterica* LPS or *S.* Typhi were measured using the quantitative enzyme-linked immunosorbent assay (ELISA) as described previously [32]. Antibody concentrations were calculated based on absorbance values and the standard curve.

Statistical analysis

Data were analyzed using GraphPad Prism 9 software (Graph Software, San Diego, CA) by multiple unpaired t-tests or two-way ANOVA followed by Tukey's multiple-comparison post-test. Kaplan–Meier survival curve comparisons were calculated by comparing two groups at each time point through the log-rank (Mantel-Cox) test. The data were expressed as the means ± SD. $P < 0.05$ was considered statistically significant.

Results

Construction of suicide vectors bearing polysaccharide biosynthetic gene clusters

As an example of chromosomal-level large DNA fragment genetic manipulation, we directly replaced the O-antigen gene cluster of *E. coli* W3110 with the O-antigen gene cluster of *S.* Typhimurium, *S.* Enteritidis, *S.* Paratyphi A, and the Vi capsular *viaB*_locus of *S.* Typhi, respectively. The sizes of these gene clusters range from 15 to 20 kbp (Supplementary Fig. S1). To construct pRE112 suicide vectors carrying such large gene clusters (Fig. 1), we used the Gibson assembly method to assemble multiple cloned fragments end to end in vitro. All the assembled products were electroporated into χ7232 and later screened by colony PCR. The successfully constructed plasmids were electroporated into χ7213 for later conjugation experiments. A detailed description of the construction processes, including each primer pair used, can be found in the supplementary methods and Fig S2-S6.

Chromosomal insertion of large gene clusters into *E. coli* W3110

Suicide vector-mediated allelic exchange was applied to insert the heterologous polysaccharide gene clusters into *E. coli* W3110 chromosome. Two strategies were used according to the requirement of an antibiotic resistance genes-cleaned background and the convenience of straightforward gene cluster replacement. One strategy resulted in scarless insertion mutations, while the other left behind a single FRT scar. A general outline of our method was shown in Fig. 2.

As an example of the first strategy, the O-antigen gene cluster of *E. coli* W3110 was precisely replaced by the *viaB*_locus of *S.* Typhi, resulting in the *E. coli* W3110 mutant L0149 (ΔOAg::*viaB*_locus). To achieve this, the suicide plasmid pHY129 (pRE112-Cm-ΔOAg::*viaB* locus) was first integrated into the chromosome of *E. coli* W3110 K028 by a first cross-over recombination through the homologous arms, either upstream or downstream. The plasmid integrate derivatives were then selected on chloramphenicol agar plates without supplemental DAP. Subsequently, a second cross-over recombination was followed to allow the excision of the suicide vector from the chromosome, and this process was counter-selected

on sucrose agar plates. Successful insertion mutants were screened by colony PCR.

As an example of the second strategy, the O-antigen gene cluster of *E. coli* W3110 was directly replaced by the heterologous O-antigen gene clusters of *S.* Paratyphi A, *S.* Typhimurium, and *S.* Enteritidis, resulting in *E. coli* W3110 mutants L0137 (Δ*wecA* ΔOAg::OAg^{SA}), L0136 (Δ*wecA* ΔOAg::OAg^{ST}), and L0133 (Δ*wecA* ΔOAg::OAg^{SE}), respectively. Similarly, after a first cross-over recombination, multiple integrants could be obtained by individually integrating the suicide plasmids pHY102 (pRE112-Km-ΔOAg::OAg^{SA}-Cm_FRT2), pHY100 (pRE112-Km-ΔOAg::OAg^{ST}-Cm_FRT2) and pHY101 (pRE112-Km-ΔOAg::OAg^{SE}-Cm_FRT2) into the chromosome of *E. coli* W3110 K062 (Δ*wecA*). Again, the suicide vector could be excised from the chromosome of the intermediate strain after a second cross-over recombination. However, unlike the first approach, this excision process was selected on sucrose plus chloramphenicol agar plates. Sucrose provided the counter-selection pressure, while chloramphenicol, due to the FRT-flanked chloramphenicol-resistant (Cm^R) cassette, would eliminate all the reversion allelic exchanges, significantly increasing the positive mutant rate. After selection, the chloramphenicol resistance gene was eliminated by a helper plasmid pCP20 encoding the FLP recombinase, leaving a single FRT scar on the chromosome.

All positive mutant strains mentioned above were sequenced by whole genome sequencing to confirm the correct insertions. The sequencing data were uploaded to NCBI as Sequence Read Archive (SRA) under accession number PRJNA1113225.

Comparison with other scarless bacteria chromosome editing techniques

The scarless insertion of large DNA segments into bacterial chromosomes is generally a challenging task. Previous studies have largely relied on the λ Red recombination system [13, 15, 37]. In this study, we employed the conjugative suicide plasmid system to achieve precise and scarless insertion of large DNA fragments. The λ Red system depends on the functions of Exo, Beta, and Gam, whereas the conjugative suicide plasmid system relies on the bacteria's endogenous RecA-dependent pathway [38]. These two methods have different homologous recombination mechanisms.

To demonstrate the speed and utility of our method, we conducted a day-by-day comparison of the conjugative suicide plasmid method with other scarless genome modification methods (Table 2). The λ Red-based method involves constructing complex plasmids each time, especially when assisted by CRISPR/Cas9. For a new insertion locus, the sgRNA target and the homology arms (HRs) must be simultaneously replaced. This process can take several days to complete unless the DNA sequence is synthesized commercially. In contrast, the conjugative suicide plasmid method is much simpler. The HRs sequences can be directly cloned from the bacterial genome and assembled in vitro with linearized suicide vectors within a single day. The main challenge lies in assembling the large gene clusters into the HRs of the suicide vectors, while other steps are routine experimental procedures.

As shown in Table 2, our method successfully inserted the largest DNA fragment with a significantly higher genetic editing efficiency (3.17×10^{-1}). Although the positive rate is slightly lower than that of the CRISPR/Cas9-assisted λ Red method, it remains above 70%, which is generally acceptable (Supplementary Fig. S7). Furthermore, the bacterial growth curves indicated no significant difference between the glycoengineered *E. coli* and their wild-type parent strain, suggesting that there is no obvious metabolic burden on the glycoengineered *E. coli* (Supplementary Fig. S8).

Heterologous polysaccharides expression from glycoengineered *E. coli* W3110 strains

In addition to the whole genome sequencing, we also evaluated the bacteria phenotype of heterologous polysaccharides by silver staining and western blot. Considering that the O-antigen polymerase Wzy and chain length determinant Wzz of *E. coli* W3110 might not recognize the Und-PP–linked O-repeat units of *S. enterica*, we transformed the pET9a-wzy^{ST} or pET9a- $(wzy\text{-}wzzB)^{ST}$ into *E. coli* W3110 mutants L0137, L0136 and L0133, resulting in L0166 (Δ*wecA* ΔOAg::OAg^{SA}, pET9a-wzy^{ST}), L0169 [Δ*wecA* ΔOAg:: OAg^{SA}, pET9a- $(wzy\text{-}wzzB)^{ST}$], L0167 (Δ*wecA* ΔOAg::OAg^{ST}, pET9a-wzy^{ST}), L0170 [Δ*wecA* ΔOAg::OAg^{ST}, pET9a- $(wzy\text{-}wzzB)^{ST}$], L0168 (Δ*wecA* ΔOAg::OAg^{SE}, pET9a-wzy^{ST}), and L0171 [Δ*wecA* ΔOAg::OAg^{SE}, pET9a- $(wzy\text{-}wzzB)^{ST}$], respectively.

Consistent with our assumptions, we did not observe apparent LPS patterns for L0137 (Δ*wecA* ΔOAg::OAg^{SA}), L0136 (Δ*wecA* ΔOAg::OAg^{ST}), and L0133 (Δ*wecA* ΔOAg::OAg^{SE}) by silver staining. Meanwhile, the deficient "rough" O-antigen phenotypes were also confirmed by western blot (Fig. 3). However, a clear LPS profile with long modal chain-length distribution was observed when complementing the wzy^{ST} and/or wzz^{ST} genes into L0136, L0133, and L0137. Furthermore, a longer chain-length modality was observed in L0169, L0170, and L0171, when compared to L0166, L0167, and L0168, respectively. Again, these distinct O-antigen polysaccharide modalities were all confirmed by western blot. In conclusion, these results indicated that: (1) Wzy^{W3110}

Table 2 Comparison of large DNA fragment chromosomal integration techniques

	Conjugative suicide plasmid	λ Red with Linear DNA donor	λ Red with plasmid DNA donor	λ Red assisted by CRISPR/Cas9
Homologous recombination mechanism	Bacterial endogenous homologous recombination system (RecA-dependent)	phage λ recombination system (Exo, Beta and Gam functions)		
Day 1	pRE112-Cm-ΔOAg or pRE112-Km-ΔOAg suicide plasmids construction (vector contained the homology arms)	pRecECA or pRecO-PS plasmid construction (pKD4 derived plasmids, featured in HR_up, MCS site, FRT-flanked-kanR cassette, and HR_down element arrangement)[1]	Construction of a donor plasmid pDOC and a helper plasmid pTKRED (pDOC featured in SceI, HR_up, gene cluster, FRT-flanked-kanR cassette, HR_down, and SceI element arrangement, and pTKRED encoding λ-red recombinase and SceI endonuclease)[2]	Construction of plasmid#1 (p15A-PBAD-Cas9PT5-Redγβα, encoding Cas9 and λ Red) and plasmid#2 (pSC101-PBAD-sgRNA-Donor, vector of sgRNA and homology arms, sgRNA targeting site flanked the homology arms)[3]
Day 2	1) Gene clusters long-range PCR; 2) Suicide plasmids PCR linearization; 3) Large suicide plasmids recombination (Gibson in vitro assembly); 4) Assembly products electroporated into c7232 host; 5) Grow transformants overnight[4]			
Day 3	1) Recombinant suicide plasmid PCR screening; 2) Slide agglutination test; 3) Extract the positive suicide plasmids; 4) Electroporate the extracted plasmids into c7213 host; 5) Grow the transformants overnight (supplement with antibiotic and DAP)	1) Gene clusters long-range PCR; 2) Gene clusters cloned into the MCS site of pRecECA or pRecO-PS; 3) Recombinant plasmids confirmation and transformation; 4) Grow transformants overnight	1) Gene clusters long-range PCR; 2) Gene clusters cloned into the MCS site of pDOC; 3) Transformation of the ligation product; 4) Electroporate pTKRED into the *E. coli* W3110; 2) Grow the cells overnight	1) Large DNA fragment PCR amplification and cloned the fragment into the homology arms of plasmid#2; 2) Electroporate plasmid#1 into *E. coli* MG1655
Day 4	Conjugational mating of c7213 transformants and *E. coli* W3110 on LB agar plates (No DAP supplement)	1) Recombinant large plasmids PCR screening; 2) Grow positive transformants overnight; 3) pKD46 electroporated into E. coli MG1655	1) Recombinant plasmids PCR screening; 2) Extract and electroporate the positive pDOC recombinant plasmids into the *E. coli* W3110 (pTKRED); 3) Grow the transformants overnight	1) Recombinant plasmid#2 PCR screening; 2) Extract and electroporate the recombinant plasmid #2 into *E. coli* MG1655 (plasmid#1)
Day 5	Scrape the mating mature and streak them on the antibiotic selection LB plate	1) Recombinant plasmids extraction; 2) Long-range PCR of HRs flanked gene clusters; 3) Electroporate linearized large *DNA* fragment into MG1655 (pKD46) cells for homologous recombination; 4) Grow transformants overnight;	1) Induced the expression of SceI endonuclease and λ-red recombinase of *E. coli* W3110 (pDOC, pTKRED) for homologous recombination; 2) Grow cells overnight	Inoculate single colonies into fresh medium for cell reproduction, and conduct genomic editing (sgRNA guides Cas9 to recognize and cleave the target DNA on MG1655 and plasmid#2. Then, the λ-Red recombinases mediate homologous recombination between the broken genome and linear donor DNA released from plasmid#2)
Day 6	1) Pick positive Colonies and inoculate them into LB broth (No antibiotic supplement); 2) Dilute the cultures and plate them on sucrose selection plates; 3) Grow overnight[5]	1) PCR screening and confirm the phenotype of the successful integrates; 2) Remove the pKD46 plasmid	1) PCR screening and confirm the phenotype of the successful integrates; 2) Remove the temperature-sensitive pTKRED plasmid and sucrose counter select against the pDOC donor plasmid;	1) PCR screening and confirm the phenotype of the successful integrates; 2) Remove the temperature-sensitive plasmid#2 and sucrose counter select against the plasmid#1

Table 2 (continued)

	Conjugative suicide plasmid	λ Red with Linear DNA donor	λ Red with plasmid DNA donor	λ Red assisted by CRISPR/Cas9
Day 7	1) Restreak colonies parallelly into LB and antibiotic-supplemented LB agar plate; 2) Perform the PCR screening against antibiotic-sensitive strains; 3) Perform the slide agglutination test against the PCR-positive strains; 4) Restreak the correct strains	1) Electroporate pCP20 plasmid into the pKD46 removed successful integrates; 2) remove the KanR cassette	1) Confirm the removal of pDOC and pTKRED plasmids; 2) Electroporate pCP20 plasmid into successful integrates; 2) Remove the KanR cassette	1) Confirm the remove of plasmid#2 and plasmid#1; 2) Restreak the correct colonies
Day 8	Store the genetically engineered strains or prepare for the other experiments	1) Confirm the sensitivity of KanR; 2) Store the genetically engineered strains or prepare for the other experiments	1) Confirm the sensitivity of KanR; 2) Store the genetically engineered strains or prepare for the other experiments	Store the genetically engineered strains or prepare for the other experiments
Result	Scarless	FRT scar	FRT scar	Scarless
Homology arm size	0.35 ~ 1.3 kb	1 ~ 1.4 kb	0.4 ~ 2.0 kb	0.5 kb
The largest DNA insert	20 kb (*S. enterica* O antigen gene cluster)[6]	9 kb (*pgl* for making a modified *C. jejuni* heptasaccharide glycan or 9-gene locus from *E. coli* O56 O antigen gene cluster)	16.3 kb (*P. aeruginosa* PAO103 O11 O antigen gene cluster)	12 kb (Fragment from the F plasmid of *E. coli* strain XL1-Blue)
Efficiency and positive rates	3.17×10^{-1} (editing efficiency); 75% (positive rate)[7]	ND[8]	ND[8]	7.2×10^{-4} (editing efficiency); 98.3% (positive rate)
Reference	This study	[15]	[13]; WO2014057109A1	[37]

[1,2,3] λ Red-based methods need to construct complicated plasmids each time, especially the plasmid#2 (replacing the sgRNA target and HRs for different insertion locus) in CRISPR/Cas9 assisting method. It would normally require several days to complete the plasmid preparation work

[4] A high-quality long-range PCR product would increase the successful Gibson in vitro assembly rate

[5] It depends on which strategy the researcher chooses. When the FRT-flanked antibiotic resistance gene was fused after the gene cluster insert, the diluted cultures could be plated on sucrose agar plates supplemented with that antibiotic. We are more likely to use the scarless strategy

[6] The largest DNA fragment we have inserted scarless on *E. coli* W3110 chromosome is around 20 Kb. We fused the $(wzy\text{-}wzzB)^{ST}$ genes right in front of the *S.* Typhimurium O antigen gene cluster and replaced the original *E. coli* W3110 O antigen locus with this rational design DNA fragment scarless, i.e., *E. coli* W3110 Δ*wecA* ΔOAg:: $(wzy\text{-}wzzB)^{ST}$- $(rmlB\text{-}wbaP)^{ST}$ insertion mutations

[7] The editing efficiency and positive rate were based on the result of supplementary Fig. S7

[8] Not disclosed

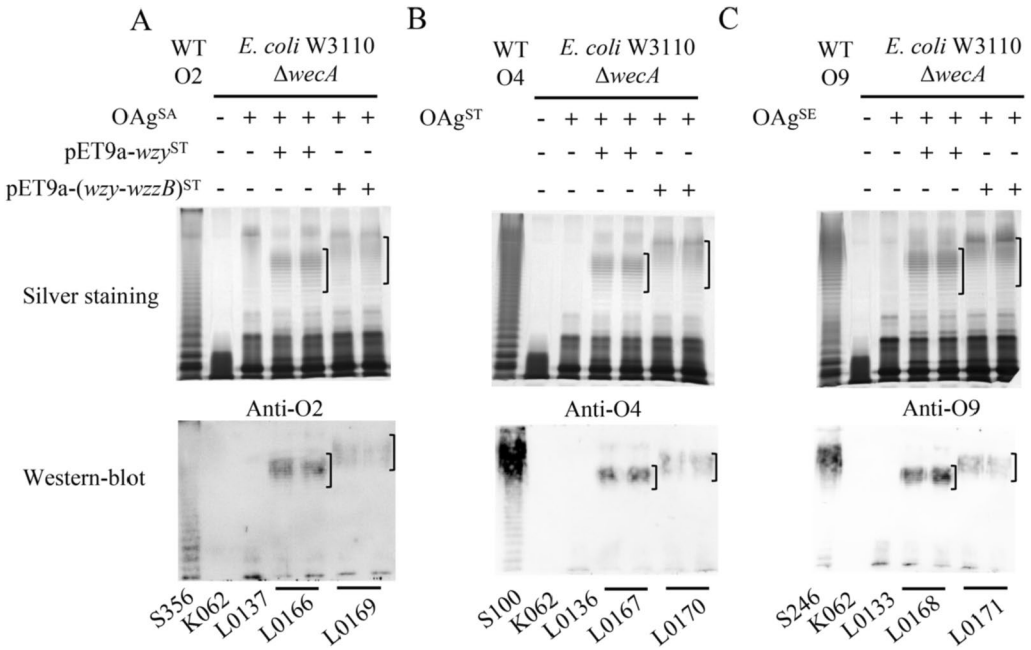

Fig. 3 The O-antigen polysaccharide (O-PS) chain-length distribution. The LPS profiles of wild-type *S.* Paratyphi A S356 (**A**), *S.* Typhimurium S100 (**B**), *S.* Enteritidis S246 (**C**), and *E. coli* W3110 Δ*wecA* derivatives are revealed by silver staining (upper panel) and western bot (lower panel). The loading samples and loading sequence are the same in each vertical group. The wild-type *S. enterica* strains show a relatively wide distribution of O-PS lengths, while no apparent O-PS pattern was observed in *E. coli* W3110 K062 (Δ*wecA*), L0137 (Δ*wecA* ΔOAg::OAg^{SA}), L0136 (Δ*wecA* ΔOAg::OAg^{ST}) and L0133 (Δ*wecA* ΔOAg::OAg^{SE}). Interestingly, *E. coli* W3110 Δ*wecA* derivatives harboring either pET9a-wzy^{ST} or pET9a- $(wzy\text{-}wzzB)^{ST}$ show a tight modal chain-length distribution (marked by left brackets) with no appreciable amounts of shorter O-PS. Meanwhile, a higher-molecular-weight modal cluster of bands is observed in pET9a- $(wzy\text{-}wzzB)^{ST}$ derivatives L0169, L0170, and L0171, when compared to their pET9a-wzy^{ST} counterpart L0166, L0167, and L0168, respectively

cannot recognize the Und-PP–linked O-repeat units of *S.* Typhimurium, *S.* Enteritidis, and *S.* Paratyphi A; (2) Wzy^{ST} could complement the function of Wzy^{SE} (Fig. 3); (3) Wzz^{ST} had a direct influence on the longer molecular size of OAg^{ST}, OAg^{ST}, and OAg^{ST} synthesis, and (4) The $WaaL^{W3110}$ ligase has broad substrate recognition, which could conjugate a non-native carbohydrate substrate assembled on Und-PP to the core oligosaccharide of lipid A. The DNA sequence of wzy^{ST} and wzy^{SA} in this study are the same (data not shown). Additionally, the modality of O-antigen chain-length in glycoengineered *E. coli* mutants and their wild-type counterparts are different. Glycoengineered *E. coli* mutants exhibited a tight modal chain-length distribution with no appreciable amounts of shorter O-antigen polysaccharides (O-PS) as indicated more clearly by the western blot results, while wild-type *S. enterica* strains had a relatively wide distribution of O-PS size (Fig. 3, lower panel). The molecular mechanism behind this phenomenon is so far unknown, which might be explained by further investigations on the detailed cooperation of Wzx, Wzy, and Wzz [39]. Furthermore, the detection of LPS in intact bacterial surface was performed by the flow cytometric analysis.

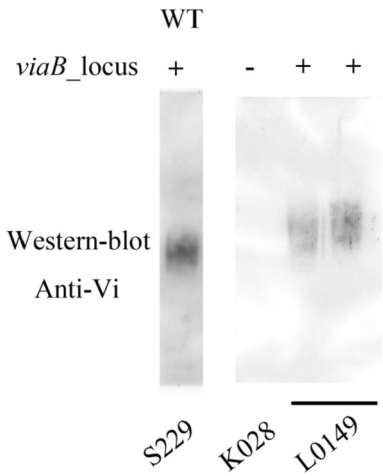

Fig. 4 Vi capsular phenotype. Western blot results of Vi capsular. Comparable amounts of Vi capsular were detected in glycoengineered *E. coli* W3110 L0149 (ΔOAg::*viaB*_locus)

and the results indicate that our glycoengineered *E. coli* could synthesize LPS efficiently and produce even larger amounts than their wild-type counterpart (supplementary Fig S9).

As for the Vi capsular, the western blot results clearly showed that the Vi capsular was expressed in *E. coli* W3110 L0149 (ΔOAg::*viaB*_locus), indicating that chromosomal insertion of *viaB*_locus is sufficient to drive the production of Vi antigen in *E. coli* (Fig. 4).

LPS yields

The potential LPS production at a relatively low cost was evaluated in M9 defined media. However, the growth curve result indicated that our glycoengineered *E. coli* strains had much lower growth rate in the M9 media when compared to the LB broth (supplementary Fig S8). Consequently, to scale up the system, modified M9 minimal media (e.g., using alternative or combined carbon or nitrogen sources) or other culture method might be needed, and their limitations or bottlenecks remains to be determined.

To evaluate the LPS production, we turned to the LB broth media. The isolated LPS products were in high purities, as no obvious protein or nucleic acid contaminants were detected by SDS-PAGE coomassie staining or spectrophotometry A260/A280 measurements (data not shown). The quantification data were summarized in Table 3. In short, the LPS yields of glycoengineered *E. coli* strains were 4 ~ 8 times less than their wild-type counterparts, and their recovery rate was around 1% of the bacterial dry weight.

Serum antibody responses to carbohydrate antigens

We next evaluated the immunogenicity of the heterologously expressed carbohydrate antigens. In light of reports revealing that a longer size of polysaccharide could induce a higher immune response and provide stronger protection [40], we prepared whole-cell inactivated antigens from L0169 [Δ*wecA* ΔOAg:: OAg^{SA}, pET9a- $(wzy\text{-}wzzB)^{ST}$], L0170 [Δ*wecA* ΔOAg::OAg^{ST}, pET9a- $(wzy\text{-}wzzB)^{ST}$], L0171 [Δ*wecA* ΔOAg::OAg^{SE}, pET9a- $(wzy\text{-}wzzB)^{ST}$], and L0149 (ΔOAg::*viaB*_locus) for subsequent mice immunization experiments.

Impressively, the adjuvants had a large impact on immunological bias. Firstly, when mice were immunized with inactivated cells without adjuvant, they generated much higher levels of polysaccharide-specific IgM than IgG (Fig. 5), indicating an inefficient process of affinity maturation and isotype switching from IgM to IgG. Conversely, when mice were immunized with inactivated cells mixed with CFA for the primary immunization and later boosted twice with the same dose of inactivated cells mixed with IFA, they generated a quite lower polysaccharide-specific IgM response, which was even non-significantly different from the PBS controls. However, they generated a much higher polysaccharide-specific IgG response than either the IgM or the controls (Fig. 5), indicating the CFA/IFA adjuvant could substantially promote affinity maturation and isotype switching from IgM to IgG.

Protective efficacy of whole-cell inactivated antigens

On day 42, vaccinated mice were challenged orally with 5×10^7 CFU of *S.* Typhimurium and *S.* Enteritidis (~ 100 times the LD50) [41], or intraperitoneally with 1×10^4 CFU of *S.* Typhi and *S.* Paratyphi A (~ 100 times the LD50) [31, 41]. The results showed that the protection rates of the L0169 [Δ*wecA* ΔOAg:: OAg^{SA}, pET9a- $(wzy\text{-}wzzB)^{ST}$] and L0170 [Δ*wecA* ΔOAg::OAg^{ST}, pET9a- $(wzy\text{-}wzzB)^{ST}$] vaccinated groups were significantly higher than the control. However, the protection rates of the L0171 [Δ*wecA* ΔOAg::OAg^{SE}, pET9a- $(wzy\text{-}wzzB)^{ST}$] and L0149 (ΔOAg::*viaB*_locus) vaccinated groups were not significantly different from the control (Fig. 6). Although the non-adjuvant groups had a dominant antibody subclass of IgM and the adjuvant groups

Table 3 LPS yields for different bacterial strains

Organism	Strain	Serotype[1]	LPS yields (mg LPS / g dried cell)[2]	Recovery rate[3]
Glycoengineered *E. coli*	L0169	O2	9.38 ± 1.59	0.9%
	L0167	O4	10.49 ± 3.47	1%
	L0171	O9	11.1 ± 3.02	1.1%
Wild type	S356	O2	71.68 ± 15.88	7.1%
	S100	O4	38.97 ± 10.52	3.9%
	S246	O9	63.59 ± 18.06	6.3%

[1] Only the immunodominant O serotype was presented

[2] One-liter bacterial culture media were lyophilized and LPS were extracted and purified by the Proteinase K Digested, Phenol–Water Extraction method. After the final dialysis step, the resultant liquid was lyophilized and weighed. The LPS yield was expressed as milligrams of LPS per gram of dried cells. Values are the average of three independent replicates and the error is the standard deviation of the mean

[3] Recovery rate referred to the yield of LPS calculated as (LPS mass/bacterial dry mass) × 100%

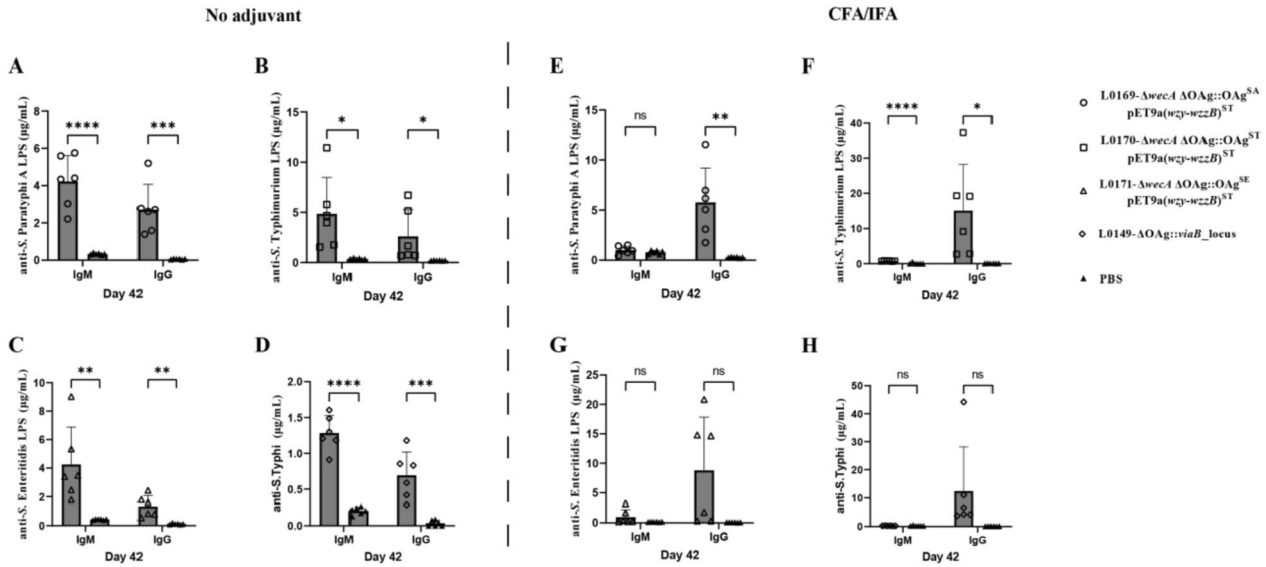

Fig. 5 Antibody responses in mice sera determined by ELISA. Anti-*S.* Paratyphi A LPS (**A**, **E**), Anti-*S.* Typhimurium LPS (**B**, **F**) and anti-*S.* Enteritidis LPS (**C**, **G**) and anti-*S.* Typhi (**D**, **H**) sera antibody concentrations in non-adjuvant (**A**-**D**) and CFA/IFA (**E**–**H**) vaccinated groups. Responses that differed from the PBS control group are noted by asterisks (*P < 0.05, **P < 0.01, ***P < 0.001, ns: non-significant difference). Antibody concentrations were calculated using a standard curve and all the measured sample concentrations were within the standard curve range. The error bars represent the standard deviations (SD) of the means calculated by the GraphPad Prism software

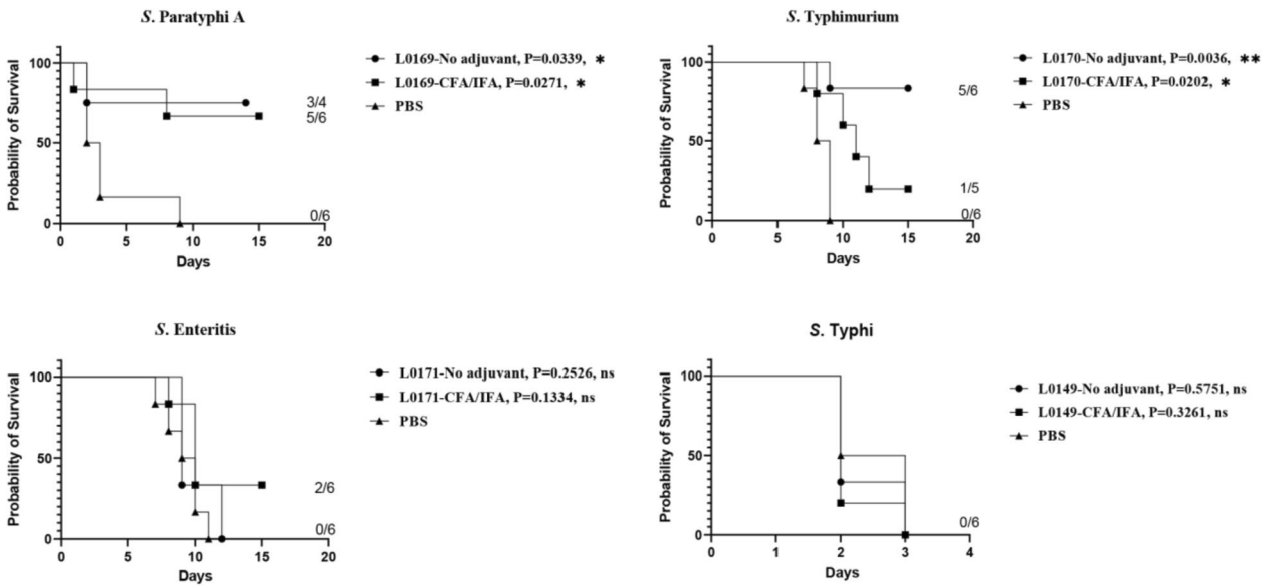

Fig. 6 Survival curves after orally or intraperitoneally challenged by wild-type *S. enterica* virulent strains. Six weeks after vaccination, BALB/c mice were challenged by about 100 times the LD50 of wild-type virulent *S.* Paratyphi A (**A**), *S.* Typhimurium (**B**), *S.* Enteritidis (**C**), and *S.* Typhi (**D**). *P < 0.05, **P < 0.01, ns: non-significant difference, for all marked groups versus the PBS control

had IgG, there was no significant difference in protection rate between these two groups.

Discussion

Bacterial surface carbohydrates, such as O-antigen and capsular polysaccharides, are excellent protective antigens [6]. The conventional approach to obtaining these polysaccharides is to extract them directly from the native pathogenic bacteria [8]. However, this strategy

has many disadvantages. Pathogenic bacteria may be difficult to cultivate, have high cultivation costs, and pose biosafety risks. Instead, carbohydrate antigen production in engineered non-pathogenic *E. coli* is much safter, cheaper and more scalable [15].

Previous research on large DNA chromosomal-level insertions was predominantly depended on the λ Red recombination system (Table 2). When aiming for scarless insertion mutations, researchers had to combine the λ Red system with the CRISPR/Cas system or other counter-selection techniques, which made the entire genetic engineering process complex and cumbersome. Although suicide plasmids with RecA-based recombination are quite common in genetic manipulations, they are mostly designed for comparatively short DNA fragment deletions or insertions [42]. Few expertise had been documented using the suicide plasmids for large DNA fragment insertions [28]. In this study, we have extended this widely used conjugative suicide plasmid method and demonstrated its feasibility in manipulating the currently challenging large DNA fragment insertions (> 15 Kbp). Unlike previously strategies, this system does not rely on endonuclease [13] or CRISPR/Cas system [37] to release the linearized DNA insert and λ-red recombinase to promote its homologous recombination. However, unintended events do exist. For example, we frequently observed the counter selection failure during the second homologous recombination, i.e., clones grown on media containing the counter-selective sucrose were frequently found to be resistant to the antibiotic marker, which indicated the plasmid backbone still remained in bacterial chromosome. We presumed that it might be spontaneous mutations of the *sacB* gene or the others that could lead to the counter selection failure. Consequently, a dual-negative selection strategy could be helpful to overcome these potential unintended events [42]. Meanwhile, our method is not limited to the commonly used *E. coli* K12 strains, i.e., W3110 or MG1655. Other recipients that could be conjugated by the χ7213 or the other donor stains are also applicable. Additionally, the insert DNA can be any large fragment, either a specific biosynthetic pathway or the genome of a virus, depending on the objective of the experiment. The only bottleneck of this method is to assemble the large DNA fragment into a suicide vector in advance.

Our strategies relied heavily on long-range PCR amplification, which might introduce random mutations and influence the polysaccharide phenotype of the mutants. Therefore, we sequenced all the positive glycoengineered *E. coli* strains by whole genome sequencing (SRA database Accession No. PRJNA1113225). Indeed, we found some random mutations, but they were all nonsense mutations. To further confirm our conclusions, we conducted bacterial growth assays, which showed no significant metabolic burden associated with the insertion of large gene clusters into the *E. coli* W3110 O-antigen locus. Additionally, to test the genetic stability of the glycoengineered *E. coli* strains, we conducted serial dilution and passage experiments. Specifically, we diluted the overnight culture 1:100 into fresh LB broth and incubated them at 37 °C with shaking until the mid-log phase. This dilution and incubation process was repeated to passage the bacteria for over 50 generations. At each passage, we collected culture samples and performed PCR to verify genetic stability. The results showed that the chromosomal integration mutations were stably maintained (data not shown). We evaluated the phenotype of the glycoengineered *E. coli* strains using silver staining, western blot, and flow cytometric analysis of intact bacteria. All these results showed that the heterologous polysaccharides were all successfully expressed.

We were interested in obtaining the polysaccharide products in a relatively high yields and at a relatively low cost. Initially, we used the M9 defined media to evaluate the growth rate of our glycoengineered *E. coli* strains. Unfortunately, glycoengineered *E. coli* did not grow as well in M9 media as it did in LB broth (Supplementary Fig S8). Therefore, the limitations and bottlenecks of large-scale culturing at a relatively low cost remain to be determined in the future. Using the proteinase K digested, phenol–water extraction method, we successfully measured the LPS production and calculated the recovery rate (Table 3). The data demonstrated that, although less efficiently than their wild-type counterparts, glycoengineered *E. coli* strains are capable of synthesizing heterologous polysaccharides with a recovery rate around 1% of the bacterial dry weight. This recovery rate is comparable to the LPS yield rate (via the phenol-water method) reported by Darveau and Hancock [43]. This result highlights the potential of glycoengineering *E. coli* as a safe platform for producing target polysaccharide products.

It is worth mentioning that the initiation synthesis of O antigen is different between *S. enterica* and *E. coli* in this study [20]. The WbaP glycosyltransferase determinates the galactose (Gal)-initiated O antigen synthesis in *S.* Typhimurium, *S.* Enteritidis, and *S.* Paratyphi A [41], while the WecA glycosyltransferase determinates the *N*-acetyl glucosamine (GlcNAc) or *N*-acetyl galactosamine (GalNAc)-initiated O antigen and Enterobacterial common antigen (ECA) synthesis in *E. coli*. WbaP and WecA attach different sugars (Gal versus GlcNAc or GalNAc) to the Und-PP and therefore would compete for the lipid carrier [44, 45]. Consequently, we derived all the O antigen heterologous expression mutants from the *E. coli* W3110 K062 (Δ*wecA*) parent strain to minimize the

Und-PP competition effect. As the Vi capsular polysaccharides are synthesized by an ABC transporter-dependent biosynthetic pathway and utilize a unique lipid anchor [46], which is distinct from lipid A, for attachment to the bacterial surface, we directly expressed the Vi capsular on the background of *E. coli* W3110 without considering deleting *waaL* and/or *wecA* right now.

In this study, the dominant protective O-epitopes O2, O4, and O9, which correspond to the paratose, abequose, and tyvelose side-branch sugars of *S.* Typhimurium, *S.* Enteritidis, and *S.* Paratyphi A O-antigen polysaccharide [41, 47], respectively, were confirmed by western blot (Fig. 3). However, detailed chemical structures of these heterologously expressed polysaccharides were not analyzed. For example, the galactose of O-antigen trisaccharide backbone can be variably glucosylated, and the C-2 position of abequose can be variably O-acetylated in *S.* Typhimurium [48]. The native variations could all generate new O-epitopes that might contribute to protective immune responses [49]. However, we cannot assure that the genes responsible for these sugar modifications are within the biosynthetic gene clusters, nor can ascertain that new irrelevant non-protective epitopes were not generated due to the heterologous expression in *E. coli*. Notably, the Vi antigen is a polymer of α- (1 → 4)-linked Nacetylgalactosaminuronic acid (GalNAcA) residues that are nonstoichiometrically O-acetylated at C-3, and the O-acetyl groups are the dominant protective epitope of the Vi antigen [50]. Although the enzyme responsible for Vi antigen O-acetylation is so far unknown, evidence has been reported that the recombinant *viaB*_locus is sufficient to drive the production of O-acetylated Vi antigen in *E. coli* [51].

To evaluate the immunogenicity of the polysaccharides expressed by our glycoengineered *E. coli* strains, we vaccinated mice with whole cell inactivated bacteria either with or without adjuvant. The results showed that much higher anti-polysaccharides IgG responses were observed in mice vaccinated with the classic strategy of mixing inactivated bacteria with CFA for the primary immunization and IFA for later booster. In contrast, the IgM subclass was the dominate antibody immune response in the non-adjuvant vaccination groups, indicating that adjuvants have a direct impact on affinity maturation and isotype switching. We suppose that the fully activated dendritic cells (DC) cells are the key factor in this switching process. When whole-cell inactivated bacteria are vaccinated with CFA, the adjuvant fully activates surrounding DC cells. These activated DC cells then migrate to nearby lymph nodes, helping activate helper T cells. Subsequently, the activated helper T cells stimulate B cells primed by the whole-cell inactivated bacteria, leading to activated B cells producing IgG antibodies. In contrast, without adjuvants, whole-cell inactivated bacteria cannot fully activate DC cells. Consequently, helper T cell activation is impaired, and antibody class-switch process of B cells is blocked. Moreover, polysaccharides, featured by their numerous repeating B cell epitopes, can naturally activate B cells through a T cell-independent pathway, resulting in dominant IgM production.

The protective rate was not significantly different between the adjuvant and non-adjuvant vaccination groups. Vaccinated mice could survive a 100 times LD50 challenge of wild type *S.* Typhimurium and *S.* Paratyphi A but succumbed to the same dose of wild type *S.* Enteritidis and *S.* Typhi. The anti-S. Enteritis LPS and anti-S. Typhi IgG immune responses were not significantly different from the PBS control group (Fig. 5G, H), showing a high degree of serum responses dispersion, and this counterintuitive result might account for the low protective rate observed in the wild type-*S.* Enteritis and *S.* Typhi challenge group. Meanwhile, we are not sure whether a > 52% O-acetylation rate occurred in Vi capsular expressed by our glycoengineered *E. coli*, and this level is recommended as a sufficient O-acetylation rate for conferring protection against typhoid fever. [52].

Importantly, our glycoengineered *E. coli* can serve as a platform for the biosynthesis of future glycoconjugate vaccines or the production of polysaccharide-based diagnostic reagents [53–55]. For example, researchers could replace the O-antigen ligase WaaL with other homologues, such as oligosaccharyltransferases PglB, PglL, PglS, etc. When transformed with plasmids expressing their target carrier protein, these glycoengineered *E. coli* could become an automated polysaccharide-protein conjugate biosynthesis platform. These glycoconjugates could be conveniently purified using His-tag affinity chromatography and/or Size Exclusion Chromatography. The manufacturing cost would be significantly reduced compared to the currently used chemical conjugation method. Another example is the potential to produce glycoengineered minicells or OMVs. Many pathogens are difficult to culture and pose biosafety concerns. Therefore, glycoengineered *E. coli* provides an alternative strategy for producing these low-cost minicells or OMVs bioproducts. By reconstructing the outer membrane polysaccharides and proteins on a model *E. coli* K12 strain, researchers can cultivate them on a large scale with minimal biosafety concerns.

Conclusion

In summary, we have extended the widely used conjugative suicide plasmid method to handle the challenging task of large DNA fragment chromosomal insertions (> 15 Kbp) and demonstrated its feasibility in non-pathogenic *E. coli* glycoengineering. Glycoengineered *E. coli*

holds significant promise in producing heterologous polysaccharides with relatively high yields and at a relatively low cost, without the potential risks of biosafety issues. More importantly, our glycoengineered *E. coli* can directly serve as a versatile platform for the production of next-generation biomedical agents. These include glycoconjugate vaccines, glycoengineered minicells or outer membrane vesicles (OMVs), polysaccharide-based diagnostic reagents, and more.

Supplementary Information

The online version contains supplementary material available at https://doi.org/10.1186/s12934-025-02749-2.

Supplementary material 1.

Supplementary material 2.

Author contributions

CX L: Data curation, Formal analysis, Methodology, Software, Validation, Writing—original draft, Writing—review and editing. HX Z, ZY J, KY W, HY G and FY L: Data curation, Formal analysis, Methodology, Validation, Visualization. ZY Z: Project administration, Resources, Supervision. HY L and P L: Conceptualization, Funding acquisition, Project administration, Resources, Supervision, Validation, Writing—original draft, Writing—review and editing.

Funding

This work was supported by the National Natural Science Foundation of China (Grant No. 32300736), the Natural Science Foundation of Chongqing, China (Grant No. CSTB2024NSCQ-MSX1157), and Fundamental Research Funds for the Central Universities (Grant No. SWU-KT23010).

Availability of data and materials

The raw sequence data can be accessed in the National Center for Biotechnology Information through SRA accession number PRJNA1113225.

Declarations

Ethics approval and consent to participate

Animal experiments were conducted in compliance with the Animal Welfare Act and regulations stated in the Guide for the Care and Use of Laboratory Animals, which was approved by the Institutional Animal Care and Use Committee of Southwest University (Approval No. LAC2024-1-0187).

Competing interests

The authors declare no competing interests.

Received: 12 February 2025 Accepted: 16 May 2025
Published online: 28 May 2025

References

1. Sande C, Whitfield C. 2021. Capsules and extracellular polysaccharides in Escherichia coli and Salmonella. EcoSal Plus 9:eESP-0033-2020.
2. Whitfield C, Wear SS, Sande C. Assembly of bacterial capsular polysaccharides and exopolysaccharides. Annu Rev Microbiol. 2020;74:521–43.
3. Whitfield C, Williams DM, Kelly SD. Lipopolysaccharide O-antigens—bacterial glycans made to measure. J Biol Chem. 2020;295:10593–609.
4. Domínguez-Medina CC, Pérez-Toledo M, Schager AE, Marshall JL, Cook CN, Bobat S, Hwang H, Chun BJ, Logan E, Bryant JA, Channell WM, Morris FC, Jossi SE, Alshayea A, Rossiter AE, Barrow PA, Horsnell WG, MacLennan CA, Henderson IR, Lakey JH, Gumbart JC, López-Macías C, Bavro VN, Cunningham AF. Outer membrane protein size and LPS O-antigen define protective antibody targeting to the Salmonella surface. Nat Commun. 2020;11:851.
5. Wilson RP, Winter SE, Spees AM, Winter MG, Nishimori JH, Sanchez JF, Nuccio S-P, Crawford RW, Tükel Ç, Bäumler AJ. The Vi capsular polysaccharide prevents complement receptor 3-mediated clearance of *Salmonella enterica* serotype Typhi. Infect Immun. 2011;79:830–7.
6. Micoli F, Costantino P, Adamo R. Potential targets for next generation antimicrobial glycoconjugate vaccines. FEMS Microbiol Rev. 2018;42:388–423.
7. Gilchrist SAN, Nanni A, Levine O. Benefits and effectiveness of administering pneumococcal polysaccharide vaccine with seasonal influenza vaccine: an approach for policymakers. Am J Public Health. 2012;102:596–605.
8. Pichichero ME. Protein carriers of conjugate vaccines: characteristics, development and clinical trials. Hum Vaccines Immunother. 2013;9:2505–23.
9. Leibeling M, Werz DB. Carbohydrate-based synthetic chemistry in the context of drug design. In: Seeberger PH, Rademacher C, editors. Carbohydrates as drugs. Cham: Springer International Publishing; 2014. p. 1–21.
10. Li W, McArthur JB, Chen X. Strategies for chemoenzymatic synthesis of carbohydrates. Carbohydr Res. 2019;472:86–97.
11. Weyant KB, Mills DC, DeLisa MP. Engineering a new generation of carbohydrate-based vaccines. Curr Opin Chem Eng. 2018;19:77–85.
12. Feldman MF, Mayer Bridwell AE, Scott NE, Vinogradov E, McKee SR, Chavez SM, Twentyman J, Stallings CL, Rosen DA, Harding CM. A promising bioconjugate vaccine against hypervirulent *Klebsiella pneumoniae*. Proc Natl Acad Sci. 2019;116:18655–63.
13. Ravenscroft N, Braun M, Schneider J, Dreyer AM, Wetter M, Haeuptle MA, Kemmler S, Steffen M, Sirena D, Herwig S, Carranza P, Jones C, Pollard AJ, Wacker M, Kowarik M. Characterization and immunogenicity of a Shigella flexneri 2a O-antigen bioconjugate vaccine candidate. Glycobiology. 2019;29:669–80.
14. Sun P, Pan C, Zeng M, Liu B, Liang H, Wang D, Liu X, Wang B, Lyu Y, Wu J, Zhu L, Wang H. Design and production of conjugate vaccines against S. Paratyphi A using an O-linked glycosylation system in vivo. Npj Vaccines. 2018;3:4.
15. Yates LE, Natarajan A, Li M, Hale ME, Mills DC, DeLisa MP. Glyco-recoded Escherichia coli: Recombineering-based genome editing of native polysaccharide biosynthesis gene clusters. Metab Eng. 2019;53:59–68.
16. Natarajan A, Jaroentomeechai T, Li M, Glasscock CJ, DeLisa MP. Metabolic engineering of glycoprotein biosynthesis in bacteria. Emerg Top Life Sci. 2018;2:419–32.
17. Samuel G, Reeves P. Biosynthesis of O-antigens: genes and pathways involved in nucleotide sugar precursor synthesis and O-antigen assembly. Carbohydr Res. 2003;338:2503–19.
18. Kalynych S, Morona R, Cygler M. Progress in understanding the assembly process of bacterial O-antigen. FEMS Microbiol Rev. 2014;38:1048–65.
19. Liu B, Knirel YA, Feng L, Perepelov AV, Senchenkova SN, Reeves PR, Wang L. Structural diversity in *Salmonella* O antigens and its genetic basis. FEMS Microbiol Rev. 2014;38:56–89.
20. Reeves PR, Cunneen MM, Liu B, Wang L. Genetics and evolution of the Salmonella galactose-initiated set of o antigens. PLoS ONE. 2013;8:e69306.
21. Ma Z, Zhang H, Li L, Chen M, Wang PG. direct cloning of bacterial surface polysaccharide gene cluster for one-step production of glycoconjugate vaccine. ACS Infect Dis. 2019;5:74–8.
22. Kachroo AH, Jayaram M, Rowley PA. Metabolic engineering without plasmids. Nat Biotechnol. 2009;27:729–31.
23. Gibson DG, Smith HO, Hutchison CA, Venter JC, Merryman C. Chemical synthesis of the mouse mitochondrial genome. Nat Methods. 2010;7:901–3.
24. Blomfield IC, Vaughn V, Rest RF, Eisenstein BI. Allelic exchange in *Escherichia coli* using the *Bacillus subtilis sacB* gene and a temperature-sensitive pSC101 replicon. Mol Microbiol. 1991;5:1447–57.
25. Baudin A, Ozier-Kalogeropoulos O, Denouel A, Lacroute F, Cullin C. A simple and efficient method for direct gene deletion in Saccharomyces cerevisiae. Nucleic Acids Res. 1993;21:3329–30.
26. Datsenko KA, Wanner BL. One-step inactivation of chromosomal genes in *Escherichia coli* K-12 using PCR products. Proc Natl Acad Sci. 2000;97:6640–5.

27. Mackie A, Paley S, Keseler IM, Shearer A, Paulsen IT, Karp PD. Addition of escherichia coli K-12 growth observation and gene essentiality data to the EcoCyc database. J Bacteriol. 2014;196:982–8.
28. Roland K, Curtiss R, Sizemore D. Construction and evaluation of a Dcya Dcrp salmonella typhimurium strain expressing avian pathogenic escherichia coli O78 lps as a vaccine to prevent airsacculitis in chickens. Avian Dis. 1999;43:429.
29. Nakayama K, Kelly SM, Curtiss R. Construction of an ASD+ expression-cloning vector: stable maintenance and high level expression of cloned genes in a salmonella vaccine strain. Bio/Technology. 1988;6:693–7.
30. Dower WJ, Miller JF, Ragsdale CW. High efficiency transformation of E.coli by high voltage electroporation. Nucleic Acids Res. 1988;16:6127–45.
31. Li P, Liu Q, Luo H, Liang K, Han Y, Roland KL, Curtiss R, Kong Q. Bi-valent polysaccharides of Vi capsular and O9 O-antigen in attenuated salmonella typhimurium induce strong immune responses against these two antigens. Npj Vaccines. 2018;3:1.
32. Li P, Liu Q, Luo H, Liang K, Yi J, Luo Y, Hu Y, Han Y, Kong Q. O-serotype conversion in salmonella typhimurium induces protective immune responses against invasive non-typhoidal salmonella infections. Front Immunol. 2017;8:1647.
33. Hitchcock PJ, Brown TM. Morphological heterogeneity among Salmonella lipopolysaccharide chemotypes in silver-stained polyacrylamide gels. J Bacteriol. 1983;154:269–77.
34. Apicella MA. Isolation and characterization of lipopolysaccharides. In: DeLeo FR, Otto M, editors. Bacterial pathogenesis: methods and protocols. Totowa, NJ: Humana Press; 2008. p. 3–13.
35. Glasscock CJ, Yates LE, Jaroentomeechai T, Wilson JD, Merritt JH, Lucks JB, DeLisa MP. A flow cytometric approach to engineering escherichia coli for improved eukaryotic protein glycosylation. Metab Eng. 2018;47:488–95.
36. Higginson EE, Simon R, Tennant SM. Animal models for salmonellosis: applications in vaccine research. Clin Vaccine Immunol. 2016;23:746–56.
37. Huang C, Guo L, Wang J, Wang N, Huo Y-X. Efficient long fragment editing technique enables large-scale and scarless bacterial genome engineering. Appl Microbiol Biotechnol. 2020;104:7943–56.
38. Court DL, Sawitzke JA, Thomason LC. Genetic engineering using homologous recombination. Annu Rev Genet. 2002;36:361–88.
39. Maczuga N, Tran ENH, Qin J, Morona R. Interdependence of Shigella flexneri O antigen and enterobacterial common antigen biosynthetic pathways. J Bacteriol. 2022;204:e00546-e621.
40. Stefanetti G, Okan N, Fink A, Gardner E, Kasper DL. Glycoconjugate vaccine using a genetically modified O antigen induces protective antibodies to *Francisella tularensis*. Proc Natl Acad Sci. 2019;116:7062–70.
41. Li P, Zhang K, Lei T, Zhou Z, Luo H. 2022. Multiple immunodominant O-epitopes co-expression in live attenuated Salmonella serovars induce cross-protective immune responses against S. Paratyphi A, S. Typhimurium and S. Enteritidis. PLoS Negl Trop Dis 16:e0010866.
42. Cianfanelli FR, Cunrath O, Bumann D. Efficient dual-negative selection for bacterial genome editing. BMC Microbiol. 2020;20:129.
43. Darveau RP, Hancock RE. Procedure for isolation of bacterial lipopolysaccharides from both smooth and rough pseudomonas aeruginosa and salmonella typhimurium strains. J Bacteriol. 1983;155:831–8.
44. Price NL, Goyette-Desjardins G, Nothaft H, Valguarnera E, Szymanski CM, Segura M, Feldman MF. Glycoengineered Outer Membrane Vesicles: A Novel Platform for Bacterial Vaccines. Sci Rep. 2016;6:24931.
45. Valvano MA. Undecaprenyl phosphate recycling comes out of age. Mol Microbiol. 2008;67:232–5.
46. Liston SD, Ovchinnikova OG, Whitfield C. Unique lipid anchor attaches Vi antigen capsule to the surface of *Salmonella enterica* serovar Typhi. Proc Natl Acad Sci. 2016;113:6719–24.
47. Luk JM, Lindberg AA. Anti-Salmonella lipopolysaccharide monoclonal antibodies: characterization of Salmonella BO-, CO-, DO-, and EO-specific clones and their diagnostic usefulness. J Clin Microbiol. 1991;29:2424–33.
48. Slauch JM, Mahan MJ, Michetti P, Neutra MR, Mekalanos JJ. Acetylation (O-factor 5) affects the structural and immunological properties of Salmonella typhimurium lipopolysaccharide O antigen. Infect Immun. 1995;63:437–41.
49. H N, K N, T N, Ph M. Glucosylation of lipopolysaccharide in Salmonella: biosynthesis of O antigen factor 12 2 . I. Over-all reaction. J Biol Chem. 1971; 246: 3912
50. Szu SC, Li XR, Stone AL, Robbins JB. Relation between structure and immunologic properties of the Vi capsular polysaccharide. Infect Immun. 1991;59:4555–61.
51. Wetter M, Goulding D, Pickard D, Kowarik M, Waechter CJ, Dougan G, Wacker M. Molecular characterization of the viab locus encoding the biosynthetic machinery for vi capsule formation in salmonella typhi. PLoS One. 2012;7: e45609.
52. Hitri K, Kuttel MM, De Benedetto G, Lockyer K, Gao F, Hansal P, Rudd TR, Beamish E, Rijpkema S, Ravenscroft N, Bolgiano B. O-acetylation of typhoid capsular polysaccharide confers polysaccharide rigidity and immunodominance by masking additional epitopes. Vaccine. 2019;37:3866–75.
53. Lensch V, Johnson JA, Kiessling LL. Glycoconjugate vaccines: platforms and adjuvants for directed immunity. Glycobiology. 2024;34:cwae092.
54. Sorieul C, Dolce M, Romano MR, Codée J, Adamo R. Glycoconjugate vaccines against antimicrobial resistant pathogens. Expert Rev Vaccines. 2023;22:1055–78.
55. Zhu H, Rollier CS, Pollard AJ. Recent advances in lipopolysaccharide-based glycoconjugate vaccines. Expert Rev Vaccines. 2021;20:1515–38.

Publisher's Note